© 2022. Published by The Company of Biologists Ltd | Journal of Experimental Biology (2022) 225, jeb244146. doi:10.1242/jeb.244146

RESEARCH ARTICLE

Inhibiting the endocannabinoid degrading enzymes FAAH and MAGL during zebrafish embryogenesis alters sensorimotor function

Lakhan S. Khara[1,*], Md Ruhul Amin[2] and Declan W. Ali[1,3,4]

ABSTRACT

The endocannabinoid system (eCS) plays a critical role in a variety of homeostatic and developmental processes. Although the eCS is known to be involved in motor and sensory function, the role of endocannabinoid (eCB) signaling in sensorimotor development remains to be fully understood. In this study, the catabolic enzymes fatty acid amide hydrolase (FAAH) and monoacylglycerol lipase (MAGL) were inhibited either simultaneously or individually during the first ∼24 h of zebrafish embryogenesis, and the properties of contractile events and escape responses were studied in animals ranging in age from 1 day post-fertilization (dpf) to 10 weeks. This perturbation of the eCS resulted in alterations to contractile activity at 1 dpf. Inhibition of MAGL using JZL 184 and dual inhibition of FAAH/MAGL using JZL 195 decreased escape swimming activity at 2 dpf. Treatment with JZL 195 also produced alterations in the properties of the 2 dpf short latency C-start escape response. Animals treated with JZL 195 exhibited deficits in escape responses elicited by auditory/vibrational stimuli at 5 and 6 dpf. These deficits were also present during the juvenile developmental stage (8- to 10-week-old fish), demonstrating a prolonged impact to sensory systems. These findings demonstrate that eCS perturbation affects sensorimotor function, and underscores the importance of eCB signaling in the development of motor and sensory processes.

KEY WORDS: Cannabinoid, Motor, Sensory, Locomotor, Behavior

INTRODUCTION

To exert its wide array of physiological influences, the endocannabinoid system (eCS) depends on the signaling of endogenous cannabinoid compounds. The endocannabinoids (eCBs) known as anandamide (AEA) and 2-arachidonoylglycerol (2-AG) are highly lipophilic compounds that act as the natural ligands of the eCS. The eCS is involved in neurobiological processes such as neural development, the fine-tuning of neuronal connections, sensation, pain and synaptic plasticity (Guindon and Hohmann, 2009; Kano et al., 2009; Martella et al., 2016). Importantly, eCBs are produced and degraded upon physiological demand (Hussain et al., 2017). Consequently, enzymes involved in eCB synthesis and degradation tightly regulate eCS activity. The eCS enzymes N-acyl phosphatidylethanolamine phospholipase D (NAPE-PLD) and diacylglycerol lipase (DAGL) are responsible for the synthesis of AEA and 2-AG, respectively (Lu and Mackie, 2016), whereas fatty acid amide hydrolase (FAAH) and monoacylglycerol lipase (MAGL) are the primary serine hydrolase enzymes that mediate the breakdown of AEA and 2-AG, respectively (Blankman et al., 2007; Cravatt et al., 1996). Cannabinoids typically exert effects through the inhibitory G-protein-coupled cannabinoid receptors known as CB1R and CB2R (Howlett, 2005), but can also interact with additional receptors such as GPR55 and transient receptor potential (TRP) channels (Amin and Ali, 2019; Morales et al., 2017; Zimov and Yazulla, 2007). Because cannabinoid receptors contribute to motor function (Luchtenburg et al., 2019), and because TRP channels are intimately linked with sensory systems, there is a need to understand the connection between the eCS and sensorimotor processes.

Several reports indicate the significance of the eCS in motor function and its involvement in sensory systems (Luchtenburg et al., 2019; Martella et al., 2016; Muller et al., 2019; Rodríguez de Fonseca et al., 1998). Antagonism of CB1R and CB2R in zebrafish embryos reduces locomotor activity, causes motor neuron defects and alters nicotinic acetylcholine receptor expression (Sufian et al., 2019). Similar effects are seen following inhibition of the eCB catabolic enzymes FAAH and MAGL (Sufian et al., 2021). Moreover, exposure to phytocannabinoids reduces miniature endplate currents in zebrafish white muscle fibers and depresses locomotor activity (Ahmed et al., 2018; Amin et al., 2020). Mammalian studies also demonstrate that locomotor activity is altered by exposure to phytocannabinoids or cannabinoid receptor agonists (Drews et al., 2005; Taffe et al., 2015). Additionally, knockdown of *dagla* causes axonal aberrations, decreased locomotion and sensory deficits in optokinetic responses (Martella et al., 2016). Finally, phytocannabinoid exposure in zebrafish embryos reduces the responsiveness to auditory stimuli (Ahmed et al., 2018). Taken together, these findings suggest that the eCS plays an important role in sensorimotor function and the development of sensory and motor systems (Muller et al., 2019).

Despite these findings, there is still much to explore regarding how eCB signaling, particularly during early life, contributes to aspects of both motor and sensory function. To address this, our study seeks to investigate how an early perturbation of the eCS – by inhibiting the enzymes FAAH and MAGL – impacts functional sensorimotor development in young zebrafish. To do this, we used pharmacological inhibitors that are specific to FAAH and MAGL. The compound known as URB 597 is a selective FAAH inhibitor, whereas JZL 184 selectively inhibits the activity of MAGL (Long et al., 2009a; Piomelli et al., 2006). Lastly, JZL 195 is used as a dual inhibitor that simultaneously acts on both FAAH and MAGL (Long

[1]Department of Biological Sciences, CW-405 Biological Sciences Building, University of Alberta Edmonton, Alberta, Canada, T6G 2E9. [2]Department of Pharmacology, CW-405 Biological Sciences Building, University of Alberta Edmonton, Alberta, Canada, T6G 2E9. [3]Department of Physiology, CW-405 Biological Sciences Building, University of Alberta Edmonton, Alberta, Canada, T6G 2E9. [4]The Neuroscience and Mental Health Institute, CW-405 Biological Sciences Building, University of Alberta Edmonton, Alberta, Canada, T6G 2E9.

*Author for correspondence (lkhara@ualberta.ca)

L.S.K., 0000-0002-5286-6290

Received 19 February 2022; Accepted 7 April 2022

Journal of Experimental Biology (2022) 225, jeb244146. doi:10.1242/jeb.244146

List of symbols and abbreviations

2-AG	2-arachidonolglycerol
AEA	anandamide
A/V	auditory/vibrational
dpf	days post-fertilization
DAGL	diacylglycerol lipase
DMSO	dimethyl sulfoxide
eCB	endocannabinoid
eCS	endocannabinoid system
FAAH	fatty acid amide hydrolase
hpf	hours post-fertilization
LMPA	low-melting point agarose
M-cell	Mauthner cell
MAGL	monoacylglycerol lipase
NAPE-PLD	N-acyl phosphatidylethanolamine phospholipase D
TRP	transient receptor potential
TL	Tubingen Longfin

et al., 2009b). The efficacy and specificity of these compounds was recently assessed in zebrafish embryos and it was established that each of these drugs specifically reduces the activity of their respective target enzyme (Sufian et al., 2021). Previous work in rodent models using the FAAH inhibitors URB 597 and SSR411298 has established that FAAH inhibition is met with increased levels of AEA (Danandeh et al., 2018; Griebel et al., 2018), while additional work demonstrated that the MAGL inhibitors SAR127303 and JZL 184 produced increased 2-AG levels (Griebel et al., 2015; Long et al., 2009a). Furthermore, dual inhibition of both FAAH and MAGL using JZL 195 elevated both AEA and 2-AG at levels that are comparable to selective inhibition of either enzyme alone (Long et al., 2009b). These findings are indicative of overactivated eCS signaling. Thus, the goal of the present study was to investigate the developmental role of eCS signaling in locomotor and functional sensorimotor development.

MATERIALS AND METHODS

Animal care, drugs and exposure

The animals used in this study were wild-type zebrafish [*Danio rerio* (Hamilton 1822)] of the Tubingen Longfin (TL) strain. All animal housing and experimental procedures in this study were approved by the Animal Care and Use Committee of the University of Alberta (AUP 00000816) and were in compliance with the Canadian Council on Animal Care guidelines of the humane use of animals for research purposes. For breeding and egg collection, adult male and female zebrafish were placed in breeding tanks on the evening before eggs were required. The following morning, eggs were collected immediately after fertilization. Embryos and larvae were housed in a 28.5°C incubator set on a 12 h:12 h light:dark cycle. Embryos and larvae were provided with embryo medium (60 mg ml^{-1}, Instant Ocean, pH 7.0).

The pharmacological compounds used in this study (all obtained from Adooq Bioscience, Irvine, CA, USA) were the selective FAAH inhibitor URB 597 at concentrations of 1, 2, 5, 10 and 20 µmol l^{-1}, the selective MAGL inhibitor JZL 184 at concentrations of 1, 2, 5, 10 and 20 µmol l^{-1}, and the dual FAAH/MAGL inhibitor JZL 195 at exposure concentrations of 1, 2 and 5 µmol l^{-1}. Fewer concentrations of JZL 195 were used owing to it possessing similar inhibitory capabilities to the combined treatment with both URB 597 and JZL 184 (Figs S1 and S2). All compounds listed here were dissolved in dimethyl sulfoxide (DMSO) – the final DMSO concentration was 0.1%, and thus 0.1% DMSO was used as the vehicle control. The drug exposure took place immediately after egg fertilization until 24 h post-fertilization (hpf), effectively spanning from ∼0 to 24 hpf (Sufian et al., 2021). Embryos were exposed to compounds diluted in embryo medium. At 24 hpf, all exposure medium was replaced and washed several times with fresh embryo medium. Following the exposure period, animals were allowed to develop until needed for further experiments.

Spontaneous coiling activity

At 1 dpf, the assessments of spontaneous coiling activity were performed using DanioScope 1.1 (Noldus, Wageningen, The Netherlands) to analyze video recordings of embryos still encased within their chorion (de Oliveira et al., 2021; Zindler et al., 2019). Video recordings of the 1 dpf embryos were taken under a dissecting microscope connected to a high-speed camera (AOS S-PRI 1995, AOS Technologies, Dättwil, Switzerland). This activity was assessed immediately after the wash-out of exposure compounds. Spontaneous coiling activity (%) was measured to indicate the proportion of time that embryos were actively contracting, while the burst count min^{-1} represents the mean number of contractions performed by embryos averaged per minute.

Escape swimming performance

To assess swimming following a C-start escape response, individual 2 dpf embryos were positioned in the center of a 140 mm Petri dish containing embryo medium. The Petri dish was set on top of an infrared backlight source to be viewed by a Basler GenICam scanning camera (Basler acA1300-60gm) with a 75 mm f2.8 C-mount lens, provided by Noldus. Escape responses in zebrafish embryos were triggered by delivering an acute mechanical stimulus to the head of the embryo by using a thin fishing line (Berkley Fishing, Spirit Lake, IA, USA, model BGQS60C-15). Each embryo was tested alone in this open field to minimize obstacles and interactions with other fish. Swimming performance was analyzed using the movement tracking software EthoVision XT-11.5 (Noldus). Mean swimming distance (cm) and mean swimming velocity (cm s^{-1}) were analyzed when assessing escape swimming performance.

Embedded escape response assessments

To assess escape response parameters, embryos at 2 dpf were partially immobilized using 2% low-melting point agarose (LMPA) at 26–30°C. The LMPA gel was cut away from the tails of the embryos, allowing for the tail's full range of motion, while leaving the head embedded in place – similar to methods used previously (Shan et al., 2015). The embryos were immersed in embryo medium and were allowed to acclimate for 20 min. Mechanical stimuli were applied by ejecting a 15 ms pulse of 2% Phenol Red (Sigma-Aldrich) from a Picospritzer II (General Valve Corporation). The pulse was delivered through borosilicate glass micropipettes (Stutter Instrument; O.D.: 1.2 mm, I.D.: 094 mm, length: 10 cm), which were pulled using a Flaming/Brown Stutter Instrument micropipette puller (Stutter Instrument model P-97). The pipettes were positioned above the embryo's otolith, and delivered a single acute stimulus to the head, which evoked a C-start tail flip. This behavior was video recorded using the AOS S-PRI 1995 high-speed camera noted above.

Video recordings were analyzed using the motion analysis software ProAnalyst (Xcitex Inc., Woburn, MA, USA). Focusing on the C-shaped bend of the embryo's tail, the following parameters were assessed: latency to initiate C-start escape response (ms), maximum speed of tail contraction (mm ms^{-1}), maximum acceleration of tail contraction (mm ms^{-2}), angle of C-bend (deg),

Journal of Experimental Biology (2022) 225, jeb244146. doi:10.1242/jeb.244146

time to achieve maximum C-bend angle (ms) and angular velocity (deg ms^{-1}).

Assessing responsiveness to auditory/vibrational stimuli

Embryos and larvae aged 3, 4, 5 and 6 dpf were assessed for their responsiveness to auditory/vibrational (A/V) stimuli in a manner similar to previous methods (Ahmed et al., 2018; Kohashi et al., 2012). Six fish were placed into a 35×10 mm Petri dish containing embryo medium and were allowed to acclimate for 20 min prior to the application of the stimulus. The A/V stimulus was created using Audacity (version 2.2.1) to generate a sawtooth waveform audio tone of 500 Hz at 95–100 dB, and was played through a set of computer speakers (Logitech Z150, Logitech, Newark, CA, USA). C-start escapes in response to the A/V stimulus were video recorded using an AOS S-PRI 1995 high-speed camera. Upon delivering the A/V stimulus, the response rate (%) was determined as the proportion of short latency C-start escape responses that occurred within each cohort of animals.

Juvenile zebrafish between the ages of 8 and 10 weeks were also used for A/V response assessments. This experiment used an identical set-up in terms of acclimation period, stimulus delivery and video recording as the larval assessments; however, the juvenile fish were tested individually and were placed in a modified 120 ml glass specimen jar (Thermo Fisher Scientific) filled with 50 ml of 28.5°C dechlorinated water, as opposed to a Petri dish, to appropriately accommodate for the increased size of juveniles.

Statistics

All data and statistical analyses were performed using GraphPad Prism (version 9.2.0, GraphPad Software, San Diego, CA, USA). All values are reported as means±s.e.m. In most cases, one-way ANOVA followed by Dunnett's multiple comparisons test against the 0.1% DMSO vehicle control was performed to determine statistical differences (P<0.05). For comparisons of juvenile A/V responsiveness, an unpaired two-tailed t-test was performed to determine statistical differences (P<0.05).

RESULTS

Inhibition of eCB degradation enzymes reduces contractile activity in embryos

Because zebrafish motor development is known to be affected by eCS perturbation, our first assessments revolved around examining one of the earliest observable locomotor processes known as burst activity (Colwill and Creton, 2011a; de Oliveira et al., 2021). This spontaneous coiling activity provides the earliest indication of locomotor development, representing the initial formation of immature synaptic contacts between the CNS and muscle fibers at the neuromuscular junction (Grunwald et al., 1988; Saint-Amant, 2006). The experiments in the following section were replicated 4 times (N=4).

Vehicle-treated embryos exhibited a mean burst activity of 4.1±0.4% (n=93) (Fig. 1A,C,E). Treatment with 1, 2 and 5 µmol l^{-1} URB 597 did not significantly affect burst activity (Fig. 1A). However, embryos treated with 10 and 20 µmol l^{-1} URB 597 exhibited a significant reduction in burst activity at 1.7±0.3% (P<0.001, n=41) and 2.0±0.4% (P<0.01, n=60), respectively. Animals treated with 1, 2, 5, 10 and 20 µmol l^{-1} JZL 184 experienced a significant decrease in burst activity relative to the vehicle (P<0.05), with the largest reductions occurring in the 20 µmol l^{-1} JZL 184 group (2.1±0.3%, P<0.001, n=80) (Fig. 1C). These reductions appear to display a dose-dependent trend. With regards to the dual FAAH/MAGL inhibitor JZL 195, treatment with 1 µmol l^{-1} JZL 195 did not cause significant impacts to burst activity. However, treatment with 2 and 5 µmol l^{-1} JZL 195 resulted in decreased burst activity with mean activity percentages of 1.8±0.2% and 2.2±0.3% (P<0.001, n=63 and n=75), respectively (Fig. 1E).

The burst count showed a similar trend to the burst activity. Vehicle treated embryos displayed a mean count of 4.1±0.4 bursts per minute (n=93) (Fig. 1B,D,F). Treatment with 10 and 20 µmol l^{-1} URB 597 resulted in a significant reduction in mean burst count min^{-1} (2.1±0.4, P<0.01, n=41 and 2.9±0.4, P<0.01, n=60, respectively) (Fig. 1B). JZL 184 treatment resulted in a reduction in mean burst count min^{-1} in all tested concentrations (P<0.05) (Fig. 1D). Lastly, treatment with 2 and 5 µmol l^{-1} JZL 195 resulted in a significantly decreased burst count min^{-1} of 2.1±0.2 (P<0.001, n=63) and 2.9±0.4 (P<0.05, n=75), respectively (Fig. 1F).

Escape swimming is negatively impacted by MAGL inhibition and dual FAAH/MAGL inhibition

The C-shaped tail flip elicited at the onset of C-start escapes is a hardwired reflex response that is crucial for survival (Colwill and Creton, 2011b). Escape swimming begins with a C-start, followed by bursts of swimming to quickly propel the animal away from the aversive stimulus. In this next series of experiments, we analyzed the escape swimming that takes place after a C-start has been performed by 2 dpf embryos (Fig. 2A). The experiments in this section were replicated a total of 4 times (N=4). The traces in Fig. 2A outline the swimming paths taken by individual animals following a C-start escape response.

Vehicle-treated embryos displayed a mean swimming distance of 6.4±0.6 cm (n=49) (Fig. 2B,D,F). Animals exposed to URB 597 (any concentration) did not experience significant alterations to escape swimming relative to the vehicle control (P>0.05) (Fig. 2B). However, treatment with JZL 184 at concentrations equal to or greater than 5 µmol l^{-1} resulted in significantly smaller swimming distances compared with controls (Fig. 2D) (P<0.01). A 24 h treatment with JZL 195 resulted in severe reductions, with mean swimming distances ranging from 3.8±0.5 cm (P<0.001, n=38) in the 1 µmol l^{-1} JZL 195 group to values as low as 0.7±0.1 cm (P<0.001, n=38) in the 5 µmol l^{-1} treated group (Fig. 2F).

The mean velocity of escape swimming in vehicle-treated embryos was 0.30±0.03 cm s^{-1} (n=49) (Fig. 2C,E,G). URB 597 and JZL 184 treatments did not affect mean swimming velocity in a statistically significant manner (P>0.05, n=37–49) (Fig. 2C,E); however, animals treated with JZL 195 experienced significant reductions in escape swimming escape velocity (Fig. 2G). For instance, embryos treated with 1 µmol l^{-1} JZL 195 had a mean velocity of 0.19±0.02 cm s^{-1} (P<0.01, n=38), whereas animals treated with 2 and 5 µmol l^{-1} JZL 195 demonstrated mean velocities of 0.14±0.02 cm s^{-1} (P<0.001, n=37) and 0.04±0.01 cm s^{-1} (P<0.001, n=38), respectively. These results indicate that singular inhibition of FAAH does not have an effect on escape swimming at 2 dpf, whereas inhibition of MAGL alters swimming distance, and dual inhibition of FAAH/MAGL has a profound impact on escape swimming.

C-start escape properties are adversely affected primarily by dual FAAH/MAGL inhibition

Next, we investigated parameters associated with the C-start escape response evoked by mechanical stimuli. To do this, we embedded 2 dpf embryos in 2% LMPA gel to isolate the initial C-shaped contraction. Representative time-lapse photos of a C-bend response are shown in Fig. 3A. Here, we used concentrations of enzyme inhibitors that had intermediate and maximal effects on escape swimming as determined in the previous set of experiments. We

Journal of Experimental Biology (2022) 225, jeb244146. doi:10.1242/jeb.244146

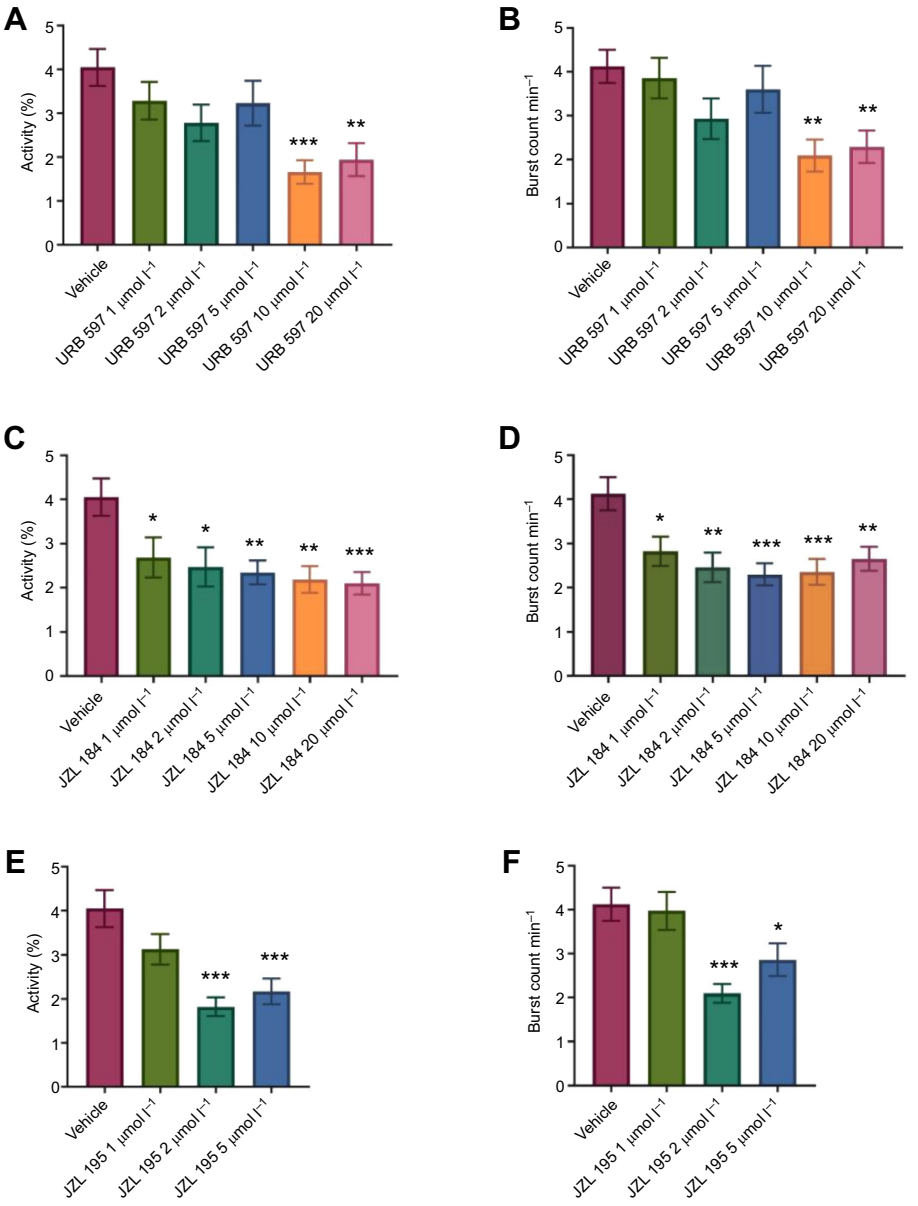

Fig. 1. Contractile activity of zebrafish embryos is reduced from inhibiting endocannabinoid degrading enzymes. Spontaneous coiling activity of embryos at the age of 1 day post-fertilization (dpf) was video-recorded and analyzed using DanioScope 1.1. (A,B) Effects on activity (%) and burst count min^{-1} for the vehicle (n=93) and treatment concentrations of 1, 2, 5, 10 and 20 µmol l^{-1} for URB 597 (n=62, 44, 58, 41 and 60, respectively). (C,D) Effects on activity (%) and burst count min^{-1} for the vehicle (n=93) and treatment concentrations of 1, 2, 5, 10 and 20 µmol l^{-1} JZL 184 (n=49, 53, 68, 54 and 80, respectively). (E,F) Effects on activity (%) and burst count min^{-1} for the vehicle (n=93) and treatment concentrations of 1, 2 and 5 µmol l^{-1} JZL 195 (n=45, 63 and 75, respectively). All treatments were run together, but for ease of viewing, the graphs are separated according to the compound being tested. Thus the vehicle controls in A, C and E are similar and the vehicles in B, D and F are similar. Activity (%) represents the proportion of time spent performing coiling movements over the recording period, while burst count min^{-1} represents the average number of individual contractions per minute. N=4 experiments with 11–23 animals per experiment for each treatment. Asterisks indicate treatment groups that are significantly different from the vehicle control group (*P<0.05, **P<0.01, ***P<0.001; one-way ANOVA, followed by Dunnett's multiple comparisons test). Error bars represent s.e.m.

then assessed parameters such as the latency of the response, peak velocity, peak acceleration, rotational angle and time to maximum bend (Figs 3 and 4). The experiments described within this section were replicated 5 times (N=5).

Vehicle treated embryos demonstrated a mean C-start response latency of 10.2±0.7 ms (n=20) (Fig. 3B). A significant increase in response latency relative to the vehicle control was seen in embryos treated with 20 µmol l^{-1} JZL 184 (13.0±1.2 ms, P<0.05, n=16) and 5 µmol l^{-1} JZL 195 (17.8±1.3 ms, P<0.001, n=15). In terms of the maximum speed of the tail during the C-bend, vehicle treated animals achieved a maximum speed of 0.23±0.01 mm ms^{-1} (n=20) (Fig. 3C) and only animals treated with 5 µmol l^{-1} JZL 195 had a reduced maximum speed of 0.29±0.02 mm ms^{-1} (P<0.05, n=15). No other treatment resulted in changes to this metric. With respect to peak acceleration of the C-bend, vehicle control embryos displayed a maximum acceleration of 0.11±0.01 mm ms^{-2} (n=20) (Fig. 3D), and the only treatment that resulted in a change to this parameter was 5 µmol l^{-1} JZL 195, where the peak acceleration was 0.08 ±0.01 mm ms^{-2} (P<0.01, n=15).

The mean rotational angle achieved by the tail was 158±9.9 deg in vehicle treated embryos (n=20) (Fig. 4A). Treatment with 5 µmol l^{-1} JZL 195 resulted in a small but significant reduction in the C-bend angle (129±6.6 deg, P<0.05, n=15). Despite this significant reduction in the angle of the C-bend caused by 5 µmol l^{-1} JZL 195, there was no significant impact on the time to complete a full C-bend (Fig. 4B). Finally, vehicle control embryos exhibited an angular velocity of 5.4±0.4 deg ms^{-1} (n=20), which was significantly reduced by 5 µmol l^{-1} JZL 195 (4.3±0.3 deg ms^{-1}, P<0.05, n=15) (Fig. 4C). These findings show that inhibition of FAAH and MAGL together leads to small effects in the C-start escape response in embryonic zebrafish.

Dual inhibition of FAAH/MAGL produces deficits to A/V responsiveness

Short latency C-start escapes also occur in response to auditory stimuli which can be evoked by delivering an A/V stimulus (Burgess and Granato, 2007; Kohashi et al., 2012). A/V stimuli-induced responses develop after 3 dpf and are functionally mature

Journal of Experimental Biology (2022) 225, jeb244146. doi:10.1242/jeb.244146

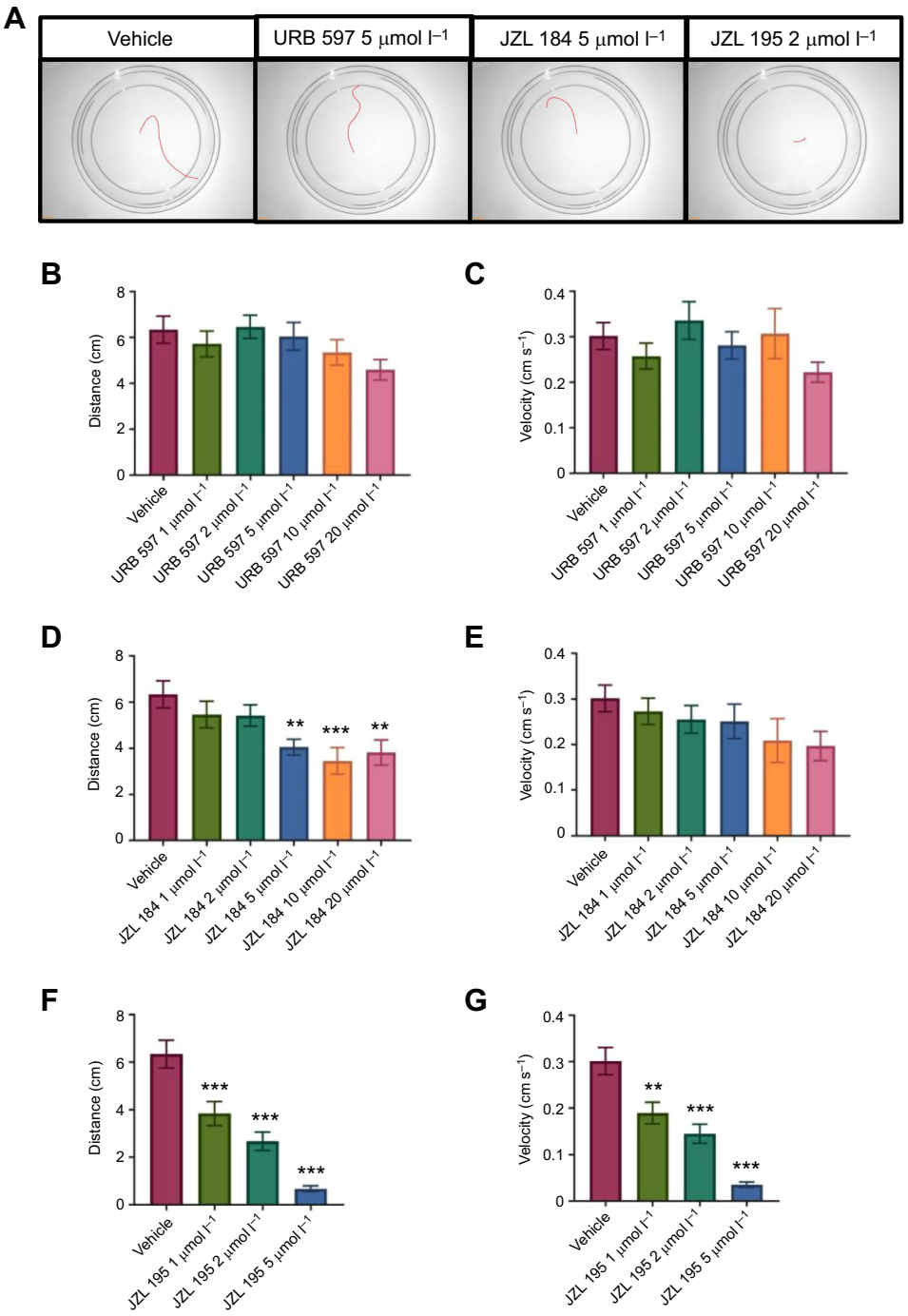

Fig. 2. Escape swimming is severely reduced by MAGL and dual FAAH/MAGL inhibition. Escape swimming at 2 dpf was assessed following an acute touch stimulus. (A) Representative tracings of the swimming path are shown for vehicle, 5 µmol l^{-1} URB 597, 5 µmol l^{-1} JZL 184 and 2 µmol l^{-1} JZL 195. (B,C) The effects of vehicle (n=49) and 1, 2, 5, 10 and 20 µmol l^{-1} URB 597 (n=39, 45, 49, 42 and 43, respectively) on swimming distance and velocity. (D,E) The effects of vehicle (n=49) and 1, 2, 5, 10 and 20 µmol l^{-1} JZL 184 (n=37, 41, 46, 40 and 40, respectively) on swimming distance and velocity. (F,G) The effects of vehicle (n=49) and 1, 2 and 5 µmol l^{-1} JZL 195 (n=38, 37 and 38, respectively) on swimming distance and velocity was analyzed using EthoVision XT-11.5. All treatments were run together, but for ease of viewing, the graphs are separated according to the compound being tested. Thus the vehicle in B, D and F are similar and the vehicle in C, E and G are similar. Swimming distance (mm) and mean velocity of burst swimming (mm s^{-1}) was examined by testing each animal individually. N=4 experiments with 9–13 animals per experiment for each treatment. Asterisks indicate treatment groups that are significantly different from the vehicle control group (**P<0.01, ***P<0.001; one-way ANOVA, followed by Dunnett's multiple comparisons test). Error bars represent s.e.m.

by 6 dpf (Kohashi et al., 2012). The experiments described here on 3 and 4 dpf animals were replicated 4 times (N=4), while experiments on 5 and 6 dpf fish were replicated 5 times (N=5).

Examining the A/V responsiveness in embryos and larvae from 3 to 6 dpf revealed that vehicle treated animals demonstrate a mean A/V escape response rate of 12.5±4.2% at 3 dpf (n=24) (Fig. 5A), and a response rate of 37.5±4.2% at 4 dpf (n=24) (Fig. 5B). There were no differences amongst any of the treatments at 3 and 4 dpf, demonstrating that at these stages, the functional development of this response proceeds normally. At 5 dpf, vehicle control larvae exhibited a mean A/V escape response rate of 80±6.2% (n=30) (Fig. 5C). Treatment with URB 597 or JZL 184 had no effect on the response rate while treatment with 2 µmol l^{-1} JZL 195 caused A/V response deficits with a mean response rate of 46.7±9.7% (P<0.05, n=30). The effect of 5 µmol l^{-1} JZL 195 was more severe at 43.3 ±4.0% (P<0.01, n=30). At 6 dpf, the responsiveness to A/V stimuli in control animals became more robust with a mean response rate of 93.3±4.0% (n=30) (Fig. 5D). Treatment with 5 or 20 µmol l^{-1} of either URB 597 or JZL 184 once again did not produce any significant alterations to A/V responsiveness, whereas treatment with 2 and 5 µmol l^{-1} JZL 195 both caused a significant decline in the responsiveness to A/V stimulus, with response rates of 60.0±11.3% (P<0.05, n=30) and 53.3±8.2% (P<0.05, n=30) for 2 and 5 µmol l^{-1} JZL 195, respectively.

Journal of Experimental Biology (2022) 225, jeb244146. doi:10.1242/jeb.244146

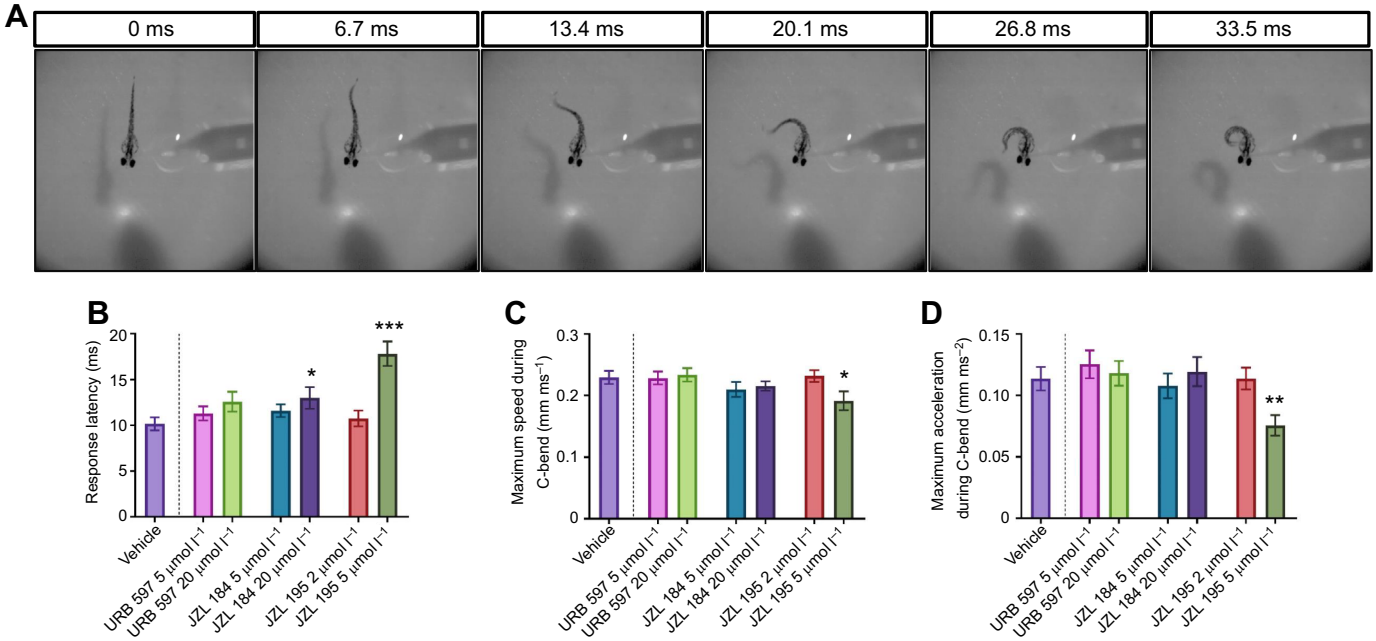

Fig. 3. C-start escape is partially altered by exposure to high concentrations of JZL 184, and is severely altered by high concentrations of JZL 195. Embryos at the age of 2 dpf were partially embedded in 2% low-melting point agarose (LMPA) and acclimated for 20 min before using a Picospritzer II to deliver an acute pulse of 2% Phenol Red solution to the head as a mechanical stimulus. (A) Representative images depicting the C-shaped tail flip performed by an immobilized vehicle control embryo after being stimulated. The time scale (ms) of the C-start is shown from its onset to its peak. (B–D) Bar graphs depict the results for vehicle control (n=20) and treatments with 5 and 20 µmol l^{-1} URB 597 (n=15 and 19), 5 and 20 µmol l^{-1} JZL 184 (n=18 and 16) or 2 and 5 µmol l^{-1} JZL 195 (n=14 and 15). The following metrics were assessed: (A) response latency (ms) to initiate C-start escape after being stimulated, (B) maximum speed achieved by the tail during the C-start escape (mm s^{-1}) and (C) maximum acceleration achieved by the tail during the C-start escape (mm s^{-2}). N=5 experiments with 3–5 animals per experiment. Asterisks indicate treatment groups that are significantly different from the vehicle control group (*P<0.05, **P<0.01, ***P<0.001; one-way ANOVA, followed by Dunnett's multiple comparisons test). Error bars represent s.e.m.

Juvenile zebrafish experience response deficits to A/V stimuli following FAAH/MAGL inhibition

To determine whether the impairments to A/V responsiveness displayed by JZL 195 treated larvae were also experienced in older animals, we raised fish into their late juvenile stages (8–10 weeks) and tested them for A/V responsiveness across three cohorts (N=3) (Fig. 6A). Animals treated with 2 µmol l^{-1} JZL 195 were tested here, as this was the minimal concentration that altered A/V

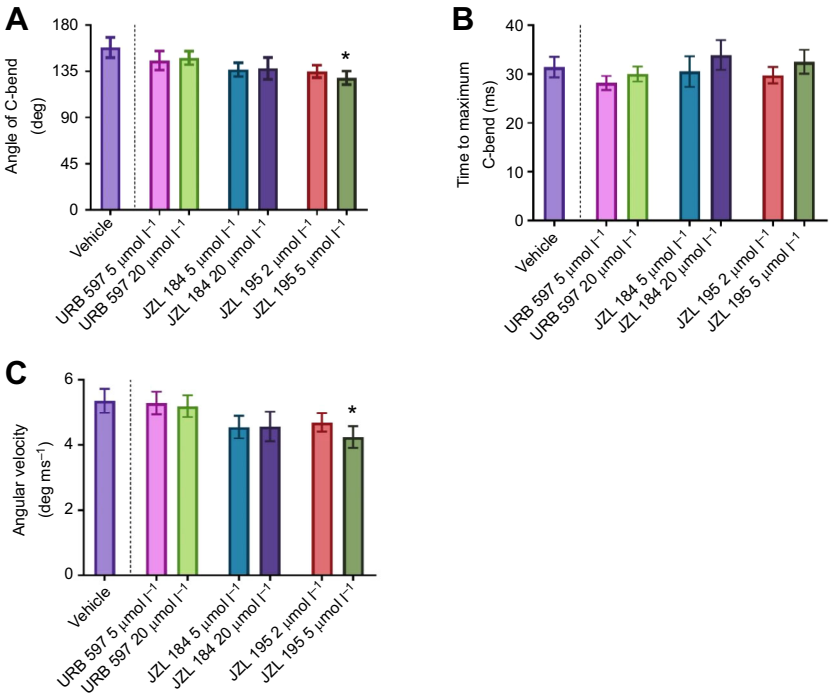

Fig. 4. Dual FAAH/MAGL inhibition produces deficits to the C-bend properties of the tail. Immobilized embryos at the age of 2 dpf were subjected to an acute mechanical stimulus and were assessed for their C-bend properties. (B–D) Bar graphs depict the results for vehicle control (n=20) and treatments with 5 and 20 µmol l^{-1} URB 597 (n=15 and 20), 5 and 20 µmol l^{-1} JZL 184 (n=18 and 17) or 2 and 5 µmol l^{-1} JZL 195 (n=15 and 15). The assessed metrics include: (A) angle of C-bend (deg), (B) length of time to achieve the maximum C-bend angle (ms) and (C) angular velocity, which represents the maximum C-bend angle over the time it takes to achieve it (deg ms^{-1}). N=5 experiments with 3–5 animals per experiment. Asterisks indicate treatment groups that are significantly different from the vehicle control group (*P<0.05; one-way ANOVA, followed by Dunnett's multiple comparisons test). Error bars represent s.e.m.

Journal of Experimental Biology (2022) 225, jeb244146. doi:10.1242/jeb.244146

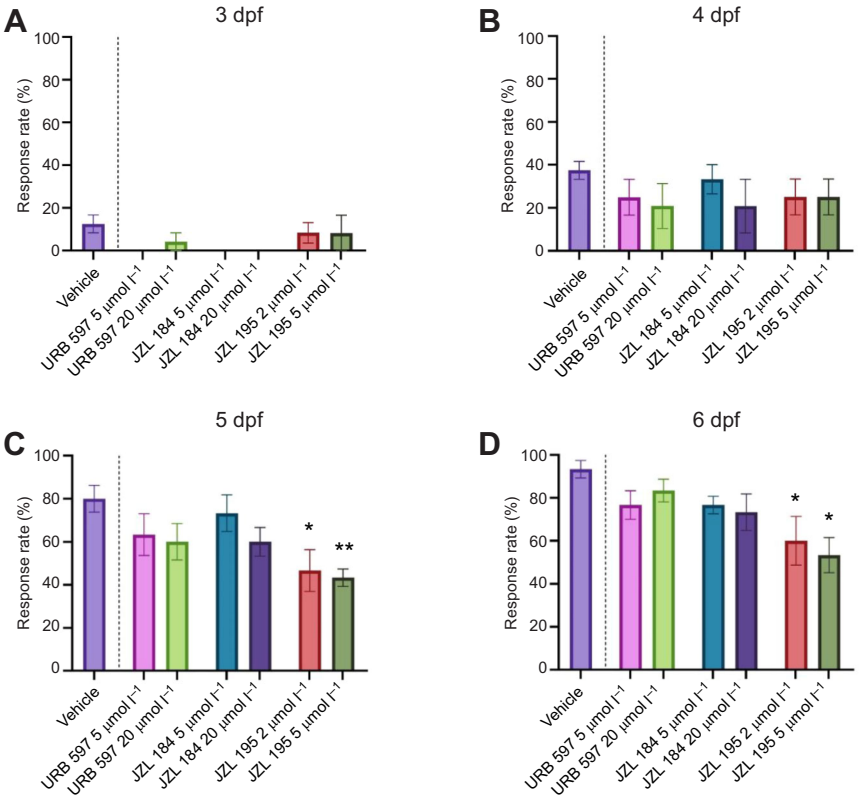

Fig. 5. Embryonic and larval responsiveness to auditory/vibrational stimuli is altered by dual FAAH/MAGL inhibition. A 500 Hz audio tone was delivered to embryos/larvae to assess their responsiveness to auditory/vibrational stimuli. Animals were tested in groups of 6 and were allowed 20 min of acclimation prior to receiving the stimulus. C-start escape responses were recorded and the proportion of responding larvae is shown as the response rate (%). Bar graphs depict the response rates for vehicle control and treatments with 5 and 20 µmol l^{-1} URB 597, 5 and 20 µmol l^{-1} JZL 184 or 2 and 5 µmol l^{-1} JZL 195 in (A) 3 dpf embryos, (B) 4 dpf larvae, (C) 5 dpf larvae and (D) 6 dpf larvae. *N*=4 experiments for 3 and 4 dpf, and *N*=5 experiments for 5 and 6 dpf with 6 animals per experiment for each treatment, thus *n*=24 for 3 and 4 dpf assessments, and *n*=30 for 5 and 6 dpf assessments. Asterisks indicate treatment groups that are significantly different from the vehicle control group (*P<0.05, **P<0.01; one-way ANOVA, followed by Dunnett's multiple comparisons test). Error bars represent s.e.m.

responsiveness at 5 and 6 dpf. Vehicle control animals demonstrated an A/V escape response rate of 85±2.6% (*n*=26) (Fig. 6B), while juvenile zebrafish that had previously been exposed to 2 µmol l^{-1} JZL 195 during embryogenesis displayed a significantly reduced response rate of 55.1±6.2% (P<0.05, *n*=25), which was similar to larval fish. This finding shows that the sensorimotor deficits caused by eCS perturbation persist into the late juvenile period of development.

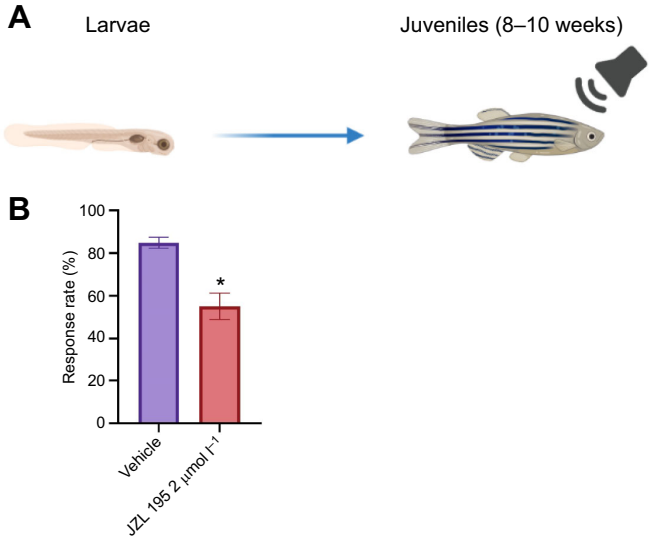

Fig. 6. The auditory/vibrational response deficits caused by dual FAAH/MAGL inhibition are present in 8- to 10-week-old juvenile zebrafish. Following the ~24 h exposure period, animals were raised to their juvenile developmental stage and were assessed individually for their responsiveness to auditory/vibrational stimuli at 8–10 weeks of age, as depicted in the schematic (A). (B) The bar graph depicts the escape response rate (%) of vehicle (*n*=26) and 2 µmol l^{-1} JZL 195 (*n*=25) treated animals. *N*=3 experiments with 7–10 animals per experiment for each treatment. Asterisks indicate treatment groups that are significantly different from the vehicle control group (*P<0.05; unpaired two-tailed *t*-test). Error bars represent s.e.m. Graphics in A were created with BioRender.com.

DISCUSSION

In this study, we found that early disruption of the eCS by blocking the activity of FAAH, MAGL or both FAAH and MAGL simultaneously during embryogenesis alters aspects of locomotor and sensorimotor function. The aim of our study was to provide a more comprehensive foundation to investigate how the eCS is involved in functional locomotor and sensorimotor development. Our results on the effects of the dual inhibitor JZL 195 show that both FAAH and MAGL activity are important for normal sensorimotor activities, as demonstrated from reduced contractile activity at 1 dpf, altered escape responses at 2 dpf, and deficits to A/V responsiveness which first appear at 5 dpf and are still present during adolescence. Singular inhibition of FAAH had little overall effect on sensorimotor function, whereas inhibition of MAGL alone resulted in small but significant effects on the development of locomotor behaviors. Importantly, our results show that the activity of both FAAH and MAGL together is essential for normal sensorimotor development, which suggests a synergistic dynamic between these two catabolic enzymes.

Our study involved using pharmacological inhibitors to disrupt eCS signaling by blocking the activity of eCB catabolic enzymes. Targeting eCB catabolic enzymes has been suggested to be a promising approach in studying the role of eCB signaling, and this has been reported in several studies using rodents (for a review, see Zou and Kumar, 2018). For example, in mice, blocking FAAH using SSR411298 caused an increase in hippocampal AEA in a dose-dependent manner, without affecting the levels of 2-AG (Griebel

et al., 2018). Additionally, similar findings are seen from administering URB 597 to rats, where blocking FAAH activity causes a significant rise in the FAAH substrates AEA, palmitoylethanolamide and oleoylethanolamide (Danandeh et al., 2018). Inhibiting MAGL activity in mice with SAR127303 substantially increases hippocampal levels of 2-AG without altering the levels of AEA (Griebel et al., 2015), while blocking MAGL with JZL 184 in mice results in an 8-fold increase in the levels of 2-AG in the brain (Long et al., 2009a). Lastly, dual inhibition of FAAH/MAGL using JZL 195 elevates the levels of both 2-AG and AEA in the brain of mice in a dose-dependent manner (Long et al., 2009b). In zebrafish, although FAAH/MAGL mediated changes in eCB levels remain to be investigated, the efficacy and specificity of the particular drugs selected in our study have previously been confirmed in zebrafish embryos (Sufian et al., 2021).

The previous reports by Sufian and colleagues focus on embryonic gross morphology, neuronal morphology and basal swimming, which represent the capacity for basic locomotor function (Saint-Amant, 2006; Sufian et al., 2021). The present study expands on this by investigating the function of sensorimotor activities such as escape responses that are elicited by specific stimuli. Importantly, the majority of activities assessed here are driven by different cues, and they represent the functionality of escape response circuits (Carmean and Ribera, 2010; Kohashi et al., 2012; Saint-Amant and Drapeau, 1998). Our findings in this report suggest a more dominant role for 2-AG signaling in zebrafish functional sensorimotor development, because few effects were observed through the individual inhibition of FAAH. However, dual FAAH/MAGL inhibition imposes the most detrimental effects on motor development, and on the sensory-driven behaviors that we examined here (Sufian et al., 2021). Previously, we also reported that exposure to these FAAH and MAGL inhibitors for the first 24 h of development resulted in reduced body lengths and morphological deformities (Sufian et al., 2021). Likewise, embryonic zebrafish exposed to cannabinoids also experience reduced body lengths, morphological aberrations, and when grown to adulthood, the females are smaller in size than age-matched controls (Ahmed et al., 2018; Pandelides et al., 2020). These findings show that cannabinoid-related morphological deformities observed during embryonic and larval development may not fully recover between the larval, juvenile and adult periods.

In zebrafish, primary motor neurons originate at ∼9 hpf during gastrulation (Westerfield et al., 1986). These developing motor axons then extend outwards from the spinal cord to innervate muscle cells. It is likely that the locomotor deficits observed at 1 and 2 dpf are partially due to motor neuron defects caused by FAAH/MAGL inhibition, which was demonstrated previously (Sufian et al., 2021). As motor neurons establish neuromuscular connections, this coincides with the formation of functional networks for locomotor activities in zebrafish (Drapeau et al., 2002). For instance, embryonic white muscle fibers play a significant role in early locomotion, as white fibers are predominantly recruited during rapid and reflexive movements, which make up the zebrafish's motor repertoire during the 1–3 dpf period of development (Buckingham and Ali, 2004; Buss and Drapeau, 2002). Meanwhile, as larval development progresses, the more tonic role of embryonic red muscle fibers further emerges, as rhythmic beat-and-glide swimming first develops between 3 and 4 dpf (Ahmed and Ali, 2016; Drapeau et al., 2002). Thus, functional motor neurons are critical for facilitating these diverse neuromuscular programs. Besides motor neurons, the transient Rohon–Beard neurons, which typically begin undergoing apoptosis after ∼34 hpf, are also known to play an important role in controlling embryonic movement in zebrafish (Slatter et al., 2005). Rohon–Beard neurons along with cerebrospinal fluid-contacting neurons are thought to control and mediate motor neuron activation in early sensorimotor processes (Henderson et al., 2019). However, it is unclear whether the eCS is involved in the development and function of these cells.

Another critical cell type developing within the first 24 h of zebrafish embryogenesis is the Mauthner cell (M-cell) and its homologs MiD2cm and MiD3cm found within the hindbrain (Kimmel et al., 1990). These large neurons, which begin developing at 8 hpf, are essential for initiating sensorimotor escape responses, and are crucial for controlling locomotor functions and for relaying incoming mechanosensory and auditory information (Bang et al., 2002). As M-cells develop, they form complex escape circuits that involve synaptic contacts with motor neurons to orchestrate rapid escape movements (Kimmel et al., 1990). In order to coordinate escape responses, when an M-cell is stimulated by mechanical or acoustic stimuli, it transmits excitatory glutamatergic signals to the contralateral motor neurons, resulting in muscular contractions that propel the animal away from the source of the stimulus (Brownstone and Chopek, 2018). Conversely, ipsilateral motor neurons are inhibited, leading to the inhibition of ipsilateral muscle fibers, which enables an agonist–antagonist muscular relationship to facilitate rapid escapes. Previous work shows that axonal growth and fasciculation of M-cells and hindbrain reticulospinal neurons is altered by knocking down the CB1R in zebrafish (Watson et al., 2008). Furthermore, embryonic exposure to Δ9-tetrahydrocannabinol reduces the diameter of M-cell axons, likely suggesting that its electrophysiological properties are altered (Amin et al., 2020). These findings highlight the importance of the eCS in M-cell development. Thus, the increased response latencies observed here may be indicative of defects in the synaptic contacts of M-cells, leading to altered M-cell-mediated communication. Because this reflex response occurs on the order of milliseconds, alterations to M-cell morphology or synaptic communications may impose deficits to escape response latency. With all this in mind, the known impacts of FAAH/MAGL inhibition on motor neurons in conjunction with the potential for effects on cell populations such as Rohon–Beard neurons and M-cells must be investigated.

Within the first 7 days of zebrafish embryonic/larval development, the inner ear undergoes a large increase in the population and density of hair cells, rendering them more sensitive to auditory stimuli (Lu and DeSmidt, 2013). Additionally, M-cells also become receptive to auditory information around ∼3 dpf, when synaptic connections between the M-cells and the otoliths become established (Bang et al., 2002). These developments are associated with increased receptiveness to auditory inputs; therefore, we sought to establish how this aspect of sensory development is functionally affected by FAAH/MAGL inhibition. We detected larval A/V response deficits in animals treated with the dual FAAH/MAGL inhibitor JZL 195, demonstrating that eCS activity is important for the development of functional auditory-escape circuits. As there was no significant effect from singular inhibition of FAAH or MAGL, our findings suggest a possible synergy between the activity of both FAAH and MAGL in the early development of auditory escape. Interestingly, significant effects of FAAH/MAGL inhibition were observed at 5 and 6 dpf, but not at 3 and 4 dpf. M-cell synaptic contacts are still undergoing early development between 3 and 4 dpf when inner ear hair cells are still at an immature stage where the sensitivity to A/V inputs is likely

low. Perhaps the escape response circuit becomes more susceptible to alterations as development proceeds and the synaptic connections become more advanced by 5 and 6 dpf. However, the exact reason for the effects being experienced at 5 and 6 dpf and not at 3 and 4 dpf is unclear at this time.

Despite being adolescent animals, juvenile zebrafish exhibit most of the adult characteristics, with the exception of male/female sexual differentiation (Parichy et al., 2009). Juveniles at ∼8 weeks of age possess functionally mature lateral line and inner ear hair cells, indicating that the auditory receptiveness of juvenile zebrafish likely reflects that of fully developed adults (Olt et al., 2014). Interestingly, despite the functional maturation of these cells, juveniles experienced the same response deficits as larval animals after treatment with JZL 195, indicating that there was no recovery from the effects of eCS perturbation on A/V responses. In mammals, CB1Rs are shown to be expressed in the cochlea (Zheng et al., 2007), while CB2Rs are expressed in inner ear hair cells and, to a lesser extent, in outer ear hair cells (Martín-Saldaña et al., 2016). Because a likely consequence of JZL 195 treatment would be the abnormal activation of cannabinoid receptors located within the inner and outer ear, it is possible that this leads to hair cell dysfunction. Furthermore, given the prevalent expression of TRPA1 and TRPV4 channels in the hair cells of the zebrafish lateral line and inner ear organs, and the known agonistic actions of eCBs with TRPA1, TRPV1 and TRPV4 (Germanà et al., 2018), eCS perturbation may impact auditory development through TRP channel interactions (Amato et al., 2012; Corey et al., 2004; Watanabe et al., 2003). Over-activation of eCS signaling likely exhibits premature and extensive activation of these receptor systems, consequently impinging upon auditory function during early life as well during later developmental stages.

Our results show that the activity of MAGL has a more significant role than FAAH in sensorimotor development, which has implications for the abundance of AEA versus 2-AG. During early development, the levels of AEA are relatively low compared with 2-AG (Fride, 2008). Furthermore, in zebrafish embryos, 2-AG is maintained at levels over 10-fold higher than AEA, indicating that 2-AG is vastly more abundant, and likely has a greater influence on receptor systems during embryogenesis (Martella et al., 2016). In terms of the cannabinoid receptors, AEA shows preferential binding towards CB1R, while 2-AG has affinity for both CB1R and CB2R (Zou and Kumar, 2018). Genetic expression of the cannabinoid receptors is present as early as 1 hpf in zebrafish, indicating that the primary eCS receptors are sensitive to the effects of eCBs within the period of our exposure paradigm (Oltrabella et al., 2017). Previous work in rodent models studying the effects of dysregulated eCB signaling found that the anxiolytic effects and locomotor alterations caused by FAAH/MAGL inhibition are prevented through blocking CB1R. In rats, the anti-anxiety effects induced by the FAAH inhibitor URB 597 can be blocked by the CB1R antagonist rimonabant (Danandeh et al., 2018; Kathuria et al., 2003). In zebrafish, the increased risk-taking and exploratory locomotor behaviors caused by the dual FAAH/MAGL inhibitor JZL 195 was partially blocked by treatment with the CB1R antagonist SR141716A (Boa-Amponsem et al., 2019). Lastly, hypolocomotion in adult rats caused by treatment with the MAGL inhibitor JZL 184 and JZL 195 was prevented by treatment with SR141716A (Seillier et al., 2014). Interestingly, CB1Rs have been shown to co-localize with TRPV1 in mouse brain, and CB2Rs co-localize with TRPV1 in human dorsal root ganglia, further highlighting the interplay between these receptor systems and the eCS ligands (Anand et al., 2008; Cristino et al., 2006). Consequently, in terms of sensory function, because AEA and its derivatives are not limited to CB1R interactions and may also act as high-affinity agonists of TRPA1 and TRPV1, these receptor systems are of great interest for further exploration, especially given our observations in the present study (Morales et al., 2017; Muller et al., 2019). Additionally, our group has recently observed the expression of *trpv1* as early as 1 dpf in the lateral line, and in Rohon–Beard and trigeminal neurons, further highlighting its potential involvement in eCS-related sensorimotor development (Son and Ali, 2022). The receptor mechanism at work here remains to be determined and is currently under investigation by our group; however, given our current and previous findings (Sufian et al., 2021), it is likely that the sensorimotor alterations observed in our study are mediated in part by CB1R as well as TRPA1 and TRPV1.

The eCS is complex in its multifaceted involvement in homeostasis and development, and although there is more emerging work aimed towards understanding its importance within the context of cannabis, further exploring the endogenous machinery is equally important. From examining early life stages in zebrafish, our findings support the existing bodies of evidence demonstrating that the eCS plays an important role in locomotor development, and expands on this by presenting varied assessments of sensorimotor function in developing animals to establish a stronger foundation in cannabinoid biology.

Competing interests

The authors declare no competing or financial interests.

Author contributions

Conceptualization: L.S.K., M.R.A.; Methodology: L.S.K., M.R.A.; Formal analysis: L.S.K.; Investigation: L.S.K.; Writing - original draft: L.S.K.; Writing - review & editing: L.S.K., D.W.A.; Visualization: L.S.K., M.R.A.; Supervision: D.W.A.; Funding acquisition: D.W.A.

Funding

Funding was provided by the Natural Sciences and Engineering Research Council of Canada.

References

Ahmed, K. T. and Ali, D. W. (2016). Nicotinic acetylcholine receptors (nAChRs) at zebrafish red and white muscle show different properties during development: nAChRs at the Zebrafish NMJ. *Devel Neurobio* **76**, 916-936. doi:10.1002/dneu.22366

Ahmed, K. T., Amin, M. R., Shah, P. and Ali, D. W. (2018). Motor neuron development in zebrafish is altered by brief (5-hr) exposures to THC (Δ9-tetrahydrocannabinol) or CBD (cannabidiol) during gastrulation. *Sci. Rep.* **8**, 10518. doi:10.1038/s41598-018-28689-z

Amato, V., Viña, E., Calavia, M. G., Guerrera, M. C., Laurà, R., Navarro, M., De Carlos, F., Cobo, J., Germanà, A. and Vega, J. A. (2012). TRPV4 in the sensory organs of adult zebrafish. *Microsc. Res. Tech.* **75**, 89-96. doi:10.1002/jemt.21029

Amin, M. R. and Ali, D. W. (2019). Pharmacology of medical cannabis. In *Recent Advances in Cannabinoid Physiology and Pathology* (ed. A. N. Bukiya), pp. 151-165. Cham: Springer International Publishing.

Amin, M. R., Ahmed, K. T. and Ali, D. W. (2020). Early exposure to THC alters M-cell development in zebrafish embryos. *Biomedicines* **8**, 5. doi:10.3390/biomedicines8010005

Anand, U., Otto, W. R., Sanchez-Herrera, D., Facer, P., Yiangou, Y., Korchev, Y., Birch, R., Benham, C., Bountra, C., Chessell, I. P. et al. (2008). Cannabinoid receptor CB2 localisation and agonist-mediated inhibition of capsaicin responses in human sensory neurons. *Pain* **138**, 667-680. doi:10.1016/j.pain.2008.06.007

Bang, P. I., Yelick, P. C., Malicki, J. J. and Sewell, W. F. (2002). High-throughput behavioral screening method for detecting auditory response defects in zebrafish. *J. Neurosci. Methods* **118**, 177-187. doi:10.1016/S0165-0270(02)00118-8

Blankman, J. L., Simon, G. M. and Cravatt, B. F. (2007). A comprehensive profile of brain enzymes that hydrolyze the endocannabinoid 2-arachidonoylglycerol. *Chem. Biol.* **14**, 1347-1356. doi:10.1016/j.chembiol.2007.11.006

Boa-Amponsem, O., Zhang, C., Mukhopadhyay, S., Ardrey, I. and Cole, G. J. (2019). Ethanol and cannabinoids interact to alter behavior in a zebrafish fetal alcohol spectrum disorder model. *Birth Defects Res.* **111**, 775-788. doi:10.1002/bdr2.1458

Brownstone, R. M. and Chopek, J. W. (2018). Reticulospinal systems for tuning motor commands. *Front. Neural Circuits* **12**, 30. doi:10.3389/fncir.2018.00030
Buckingham, S. D. and Ali, D. W. (2004). Sodium and potassium currents of larval zebrafish muscle fibres. *J. Exp. Biol.* **207**, 841-852. doi:10.1242/jeb.00839
Burgess, H. A. and Granato, M. (2007). Sensorimotor gating in larval zebrafish. *J. Neurosci.* **27**, 4984-4994. doi:10.1523/JNEUROSCI.0615-07.2007
Buss, R. R. and Drapeau, P. (2002). Activation of embryonic red and white muscle fibers during fictive swimming in the developing zebrafish. *J. Neurophysiol.* **87**, 1244-1251. doi:10.1152/jn.00659.2001
Carmean, V. and Ribera, A. B. (2010). Genetic analysis of the touch response in zebrafish (*Danio rerio*). *Int. J. Comp. Psychol.* **23**, 91.
Colwill, R. M. and Creton, R. (2011a). Locomotor behaviors in zebrafish (*Danio rerio*) larvae. *Behav. Process.* **86**, 222-229. doi:10.1016/j.beproc.2010.12.003
Colwill, R. M. and Creton, R. (2011b). Imaging escape and avoidance behavior in zebrafish larvae. *Rev. Neurosci.* **22**, 63-73. doi:10.1515/rns.2011.008
Corey, D. P., García-Añoveros, J., Holt, J. R., Kwan, K. Y., Lin, S.-Y., Vollrath, M. A., Amalfitano, A., Cheung, E. L.-M., Derfler, B. H., Duggan, A. et al. (2004). TRPA1 is a candidate for the mechanosensitive transduction channel of vertebrate hair cells. *Nature* **432**, 723-730. doi:10.1038/nature03066
Cravatt, B. F., Giang, D. K., Mayfield, S. P., Boger, D. L., Lerner, R. A. and Gilula, N. B. (1996). Molecular characterization of an enzyme that degrades neuromodulatory fatty-acid amides. *Nature* **384**, 83-87. doi:10.1038/384083a0
Cristino, L., de Petrocellis, L., Pryce, G., Baker, D., Guglielmotti, V. and Di Marzo, V. (2006). Immunohistochemical localization of cannabinoid type 1 and vanilloid transient receptor potential vanilloid type 1 receptors in the mouse brain. *Neuroscience* **139**, 1405-1415. doi:10.1016/j.neuroscience.2006.02.074
Danandeh, A., Vozella, V., Lim, J., Oveisi, F., Ramirez, G. L., Mears, D., Wynn, G. and Piomelli, D. (2018). Effects of fatty acid amide hydrolase inhibitor URB597 in a rat model of trauma-induced long-term anxiety. *Psychopharmacology* **235**, 3211-3221. doi:10.1007/s00213-018-5020-7
de Oliveira, A., Brigante, T. and Oliveira, D. (2021). Tail coiling assay in zebrafish (*Danio rerio*) embryos: stage of development, promising positive control candidates, and selection of an appropriate organic solvent for screening of developmental neurotoxicity (DNT). *Water* **13**, 119. doi:10.3390/w13020119
Drapeau, P., Saint-Amant, L., Buss, R. R., Chong, M., McDearmid, J. R. and Brustein, E. (2002). Development of the locomotor network in zebrafish. *Prog. Neurobiol.* **68**, 85-111. doi:10.1016/S0301-0082(02)00075-8
Drews, E., Schneider, M. and Koch, M. (2005). Effects of the cannabinoid receptor agonist win 55,212-2 on operant behavior and locomotor activity in rats. *Pharmacol. Biochem. Behav.* **80**, 145-150. doi:10.1016/j.pbb.2004.10.023
Fride, E. (2008). Multiple roles for the endocannabinoid system during the earliest stages of life: pre- and postnatal development. *J. Neuroendocrinol.* **20**, 75-81. doi:10.1111/j.1365-2826.2008.01670.x
Germanà, A., Muriel, J. D., Cobo, R., García-Suárez, O. and Cobo, J. (2018). Transient-receptor potential (TRP) and acid-sensing ion channels (ASICs) in the sensory organs of adult zebrafish. In *Recent Advances in Zebrafish Researches* (ed. Y. Bozkurt), pp. 101-117. InTech.
Griebel, G., Pichat, P., Beeské, S., Leroy, T., Redon, N., Jacquet, A., Françon, D., Bert, L., Even, L., Lopez-Grancha, M. et al. (2015). Selective blockade of the hydrolysis of the endocannabinoid 2-arachidonoylglycerol impairs learning and memory performance while producing antinociceptive activity in rodents. *Sci. Rep.* **5**, 7642. doi:10.1038/srep07642
Griebel, G., Stemmelin, J., Lopez-Grancha, M., Fauchey, V., Slowinski, F., Pichat, P., Dargazanli, G., Abouabdellah, A., Cohen, C. and Bergis, O. E. (2018). The selective reversible FAAH inhibitor, SSR411298, restores the development of maladaptive behaviors to acute and chronic stress in rodents. *Sci. Rep.* **8**, 2416. doi:10.1038/s41598-018-20895-z
Grunwald, D. J., Kimmel, C. B., Westerfield, M., Walker, C. and Streisinger, G. (1988). A neural degeneration mutation that spares primary neurons in the zebrafish. *Dev. Biol.* **126**, 115-128. doi:10.1016/0012-1606(88)90245-X
Guindon, J. and Hohmann, A. G. (2009). The endocannabinoid system and pain. *CNS Neurol. Disord. Drug Targets* **8**, 403-421. doi:10.2174/187152709789824660
Henderson, K. W., Menelaou, E. and Hale, M. E. (2019). Sensory neurons in the spinal cord of zebrafish and their local connectivity. *Curr. Opin. Physiol.* **8**, 136-140. doi:10.1016/j.cophys.2019.01.008
Howlett, A. C. (2005). Cannabinoid receptor signaling. *Handb. Exp. Pharmacol.* **168**, 53-79. doi:10.1007/3-540-26573-2_2
Hussain, Z., Uyama, T., Tsuboi, K. and Ueda, N. (2017). Mammalian enzymes responsible for the biosynthesis of N-acylethanolamines. *Biochim. Biophys. Acta Mol. Cell Biol. Lipids* **1862**, 1546-1561. doi:10.1016/j.bbalip.2017.08.006
Kano, M., Ohno-Shosaku, T., Hashimotodani, Y., Uchigashima, M. and Watanabe, M. (2009). Endocannabinoid-mediated control of synaptic transmission. *Physiol. Rev.* **89**, 309-380. doi:10.1152/physrev.00019.2008
Kathuria, S., Gaetani, S., Fegley, D., Valiño, F., Duranti, A., Tontini, A., Mor, M., Tarzia, G., Rana, G. L., Calignano, A. et al. (2003). Modulation of anxiety through blockade of anandamide hydrolysis. *Nat. Med.* **9**, 76-81. doi:10.1038/nm803
Kimmel, C. B., Hatta, K. and Metcalfe, W. K. (1990). Early axonal contacts during development of an identified dendrite in the brain of the zebrafish. *Neuron* **4**, 535-545. doi:10.1016/0896-6273(90)90111-R
Kohashi, T., Nakata, N. and Oda, Y. (2012). Effective sensory modality activating an escape triggering neuron switches during early development in zebrafish. *J. Neurosci.* **32**, 5810-5820. doi:10.1523/JNEUROSCI.6169-11.2012
Long, J. Z., Li, W., Booker, L., Burston, J. J., Kinsey, S. G., Schlosburg, J. E., Pavón, F. J., Serrano, A. M., Selley, D. E., Parsons, L. H. et al. (2009a). Selective blockade of 2-arachidonoylglycerol hydrolysis produces cannabinoid behavioral effects. *Nat. Chem. Biol.* **5**, 37-44. doi:10.1038/nchembio.129
Long, J. Z., Nomura, D. K., Vann, R. E., Walentiny, D. M., Booker, L., Jin, X., Burston, J. J., Sim-Selley, L. J., Lichtman, A. H., Wiley, J. L. et al. (2009b). Dual blockade of FAAH and MAGL identifies behavioral processes regulated by endocannabinoid crosstalk *in vivo*. *Proc. Natl Acad. Sci. USA* **106**, 20270-20275. doi:10.1073/pnas.0909411106
Lu, Z. and DeSmidt, A. A. (2013). Early development of hearing in zebrafish. *J. Assoc. Res. Otolaryngol.* **14**, 509-521. doi:10.1007/s10162-013-0386-z
Lu, H.-C. and Mackie, K. (2016). An introduction to the endogenous cannabinoid system. *Biol. Psychiatry* **79**, 516-525. doi:10.1016/j.biopsych.2015.07.028
Luchtenburg, F. J., Schaaf, M. J. M. and Richardson, M. K. (2019). Functional characterization of the cannabinoid receptors 1 and 2 in zebrafish larvae using behavioral analysis. *Psychopharmacology* **236**, 2049-2058. doi:10.1007/s00213-019-05193-4
Martella, A., Sepe, R. M., Silvestri, C., Zang, J., Fasano, G., Carnevali, O., De Girolamo, P., Neuhauss, S. C. F., Sordino, P. and Di Marzo, V. (2016). Important role of endocannabinoid signaling in the development of functional vision and locomotion in zebrafish. *FASEB J.* **30**, 4275-4288. doi:10.1096/fj.201600602R
Martín-Saldaña, S., Trinidad, A., Ramil, E., Sánchez-López, A. J., Coronado, M. J., Martínez-Martínez, E., García, J. M., García-Berrocal, J. R. and Ramírez-Camacho, R. (2016). Spontaneous Cannabinoid Receptor 2 (CB2) expression in the cochlea of adult albino rat and its up-regulation after cisplatin treatment. *PLoS ONE* **11**, e0161954. doi:10.1371/journal.pone.0161954
Morales, P., Hurst, D. P. and Reggio, P. H. (2017). Molecular targets of the phytocannabinoids: a complex picture. In *Phytocannabinoids* (ed. A. D. Kinghorn, H. Falk, S. Gibbons and J. Kobayashi), pp. 103-131. Cham: Springer International Publishing.
Muller, C., Morales, P. and Reggio, P. H. (2019). Cannabinoid ligands targeting TRP channels. *Front. Mol. Neurosci.* **11**, 487. doi:10.3389/fnmol.2018.00487
Olt, J., Johnson, S. L. and Marcotti, W. (2014). In vivo and in vitro biophysical properties of hair cells from the lateral line and inner ear of developing and adult zebrafish. *J. Physiol.* **592**, 2041-2058. doi:10.1113/jphysiol.2013.265108
Oltrabella, F., Melgoza, A., Nguyen, B. and Guo, S. (2017). Role of the endocannabinoid system in vertebrates: emphasis on the zebrafish model. *Dev. Growth Differ.* **59**, 194-210. doi:10.1111/dgd.12351
Pandelides, Z., Thornton, C., Faruque, A. S., Whitehead, A. P., Willett, K. L. and Ashpole, N. M. (2020). Developmental exposure to cannabidiol (CBD) alters longevity and health span of zebrafish (*Danio rerio*). *GeroScience* **42**, 785-800. doi:10.1007/s11357-020-00182-4
Parichy, D. M., Elizondo, M. R., Mills, M. G., Gordon, T. N. and Engeszer, R. E. (2009). Normal table of post-embryonic zebrafish development: staging by externally visible anatomy of the living fish. *Dev. Dyn.* **238**, 2975-3015. doi:10.1002/dvdy.22113
Piomelli, D., Tarzia, G., Duranti, A., Tontini, A., Mor, M., Compton, T. R., Dasse, O., Monaghan, E. P., Parrott, J. A. and Putman, D. (2006). Pharmacological profile of the selective FAAH inhibitor KDS–4103 (URB597). *CNS Drug Rev.* **12**, 21-38. doi:10.1111/j.1527-3458.2006.00021.x
Rodríguez de Fonseca, F., Del Arco, I., Martín-Calderón, J. L., Gorriti, M. A. and Navarro, M. (1998). Role of the endogenous cannabinoid system in the regulation of motor activity. *Neurobiol. Dis.* **5**, 483-501. doi:10.1006/nbdi.1998.0217
Saint-Amant, L. (2006). Development of motor networks in zebrafish embryos. *Zebrafish* **3**, 173-190. doi:10.1089/zeb.2006.3.173
Saint-Amant, L. and Drapeau, P. (1998). Time course of the development of motor behaviors in the zebrafish embryo. *J. Neurobiol.* **37**, 622-632. doi:10.1002/(SICI)1097-4695(199812)37:4<622::AID-NEU10>3.0.CO;2-S
Seillier, A., Aguilar, D. D. and Giuffrida, A. (2014). The dual FAAH/MAGL inhibitor JZL195 has enhanced effects on endocannabinoid transmission and motor behavior in rats as compared to those of the MAGL inhibitor JZL184. *Pharmacol. Biochem. Behav.* **124**, 153-159. doi:10.1016/j.pbb.2014.05.022
Shan, S. D., Boutin, S., Ferdous, J. and Ali, D. W. (2015). Ethanol exposure during gastrulation alters neuronal morphology and behavior in zebrafish. *Neurotoxicol. Teratol.* **48**, 18-27. doi:10.1016/j.ntt.2015.01.004
Slatter, C. A. B., Kanji, H., Coutts, C. A. and Ali, D. W. (2005). Expression of PKC in the developing zebrafish, *Danio rerio*. *J. Neurobiol.* **62**, 425-438. doi:10.1002/neu.20110
Son, H.-W. and Ali, D. W. (2022). Endocannabinoid receptor expression in early zebrafish development. *Dev. Neurosci.* **25**. doi:10.1159/000522383
Sufian, M. S., Amin, M. R., Kanyo, R., Allison, W. T. and Ali, D. W. (2019). CB1 and CB2 receptors play differential roles in early zebrafish locomotor development. *J. Exp. Biol.* **222**, jeb206680. doi:10.1242/jeb.206680
Sufian, M. S., Amin, M. R. and Ali, D. W. (2021). Early suppression of the endocannabinoid degrading enzymes FAAH and MAGL alters

locomotor development in zebrafish. *J. Exp. Biol.* **224**, jeb.242635. doi:10.1242/jeb.242635

Taffe, M. A., Creehan, K. M. and Vandewater, S. A. (2015). Cannabidiol fails to reverse hypothermia or locomotor suppression induced by Δ9-tetrahydrocannabinol in Sprague-Dawley rats. *Br. J. Pharmacol.* **172**, 1783-1791. doi:10.1111/bph.13024

Watanabe, H., Vriens, J., Prenen, J., Droogmans, G., Voets, T. and Nilius, B. (2003). Anandamide and arachidonic acid use epoxyeicosatrienoic acids to activate TRPV4 channels. *Nature* **424**, 434-438. doi:10.1038/nature01807

Watson, S., Chambers, D., Hobbs, C., Doherty, P. and Graham, A. (2008). The endocannabinoid receptor, CB1, is required for normal axonal growth and fasciculation. *Mol. Cell. Neurosci.* **38**, 89-97. doi:10.1016/j.mcn.2008.02.001

Westerfield, M., McMurray, J. V. and Eisen, J. S. (1986). Identified motoneurons and their innervation of axial muscles in the zebrafish. *J. Neurosci.* **6**, 2267-2277. doi:10.1523/JNEUROSCI.06-08-02267.1986

Zheng, Y., Baek, J.-H., Smith, P. F. and Darlington, C. L. (2007). Cannabinoid receptor down-regulation in the ventral cochlear nucleus in a salicylate model of tinnitus. *Hear. Res.* **228**, 105-111. doi:10.1016/j.heares.2007.01.028

Zimov, S. and Yazulla, S. (2007). Vanilloid receptor 1 (TRPV1/VR1) co-localizes with fatty acid amide hydrolase (FAAH) in retinal amacrine cells. *Vis. Neurosci.* **24**, 581-591. doi:10.1017/S095252380707054X

Zindler, F., Beedgen, F., Brandt, D., Steiner, M., Stengel, D., Baumann, L. and Braunbeck, T. (2019). Analysis of tail coiling activity of zebrafish (*Danio rerio*) embryos allows for the differentiation of neurotoxicants with different modes of action. *Ecotoxicol. Environ. Saf.* **186**, 109754. doi:10.1016/j.ecoenv.2019.109754

Zou, S. and Kumar, U. (2018). Cannabinoid receptors and the endocannabinoid system: signaling and function in the central nervous system. *IJMS* **19**, 833. doi:10.3390/ijms19030833